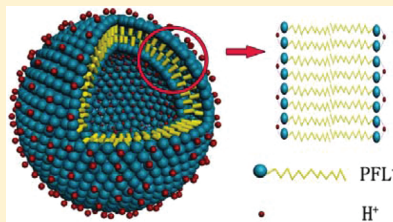


pH-Sensitive Vesicles and Rheological Properties of PFLA/NaOH/H₂O and PFLA/LiOH/H₂O Systems

Panfeng Long, Aixin Song, Dong Wang, Renhao Dong, and Jingcheng Hao*

Key Laboratory of Colloid and Interface Chemistry, Shandong University, Ministry of Education, Jinan 250100, People's Republic of China

ABSTRACT: The formation of pH-sensitive vesicles and the rheological properties of the mixtures of perfluorolauric acid (PFLA) and its salts (PFL-Na and PFL-Li) neutralized via NaOH or LiOH were investigated in aqueous solution. When the right mixing ratios of the ionized to nonionized PFLA molecules with a very high Krafft point are established, vesicles can spontaneously form at room temperature. The vesicles spontaneously formed in the PFLA/PFL-Na/H₂O system with the rigid fluorocarbon chains were determined by atomic force microscopy images. Compared to those of hydrocarbon amphiphiles, these vesicle samples, which can be kept for 2 years at room temperature, are more stable. The phase transition from the vesicle phase to the lamellar lyotropic liquid crystal phase with the increase of pH was determined by freeze-fracture transmission electron microscopy images in the PFLA/PFL-Li/H₂O system. The system of perfluoro fatty acid vesicles exhibits much more interesting rheological properties, compared to hydrocarbon fatty acid vesicles. The perfluoro fatty acid vesicle solutions display a much higher yield stress and viscoelastic properties, which depend on two factors: (i) the fluorinated alkyl chains of PFL⁻, which are in the crystalline state at room temperature because of their rigid chains compared to analogous hydrocarbon chains, and (ii) the packing of the vesicles, which is very dense. This is the first time that pH-sensitive vesicles exhibiting birefringence were constructed through ionizing perfluoro fatty acid, which may direct primarily toward acquiring an understanding of the mechanism of vesicles depending on the right mixing ratios of the ionized to the nonionized perfluoro fatty acid molecules with a very high Krafft point and secondarily to expand the development of fluorinated surfactants in both fundamental research and practical applications.



INTRODUCTION

Over recent years, surfactant scientists' interests have been focused on self-assembled aggregates formed in surfactant mixtures in solution, largely because mixed surfactant systems show more interesting phase behavior and useful properties than single components. For example, when a solution of mixed surfactants generally shows a lower surface tension and critical micelle concentration (CMC) than that of the individual component of the mixtures at the same concentration, then the mixtures are said to exhibit synergism.^{1–3} Since cationic and anionic (catanionic) surfactant mixtures were reported by Kaler et al. to form thermodynamically stable vesicles in dilute aqueous solutions in 1989,⁴ surfactant scientists have studied a number of features of catanionic surfactant mixtures, especially the vesicles formed in these systems.^{5–9}

Fatty acid vesicles are colloidal suspensions of closed bilayers that are composed of fatty acids and their ionized species. The formation of fatty acid vesicles was first discovered by Gebicki and Hicks in 1973, and the vesicles formed in oleic acid aqueous solution buffered at pH 8–9 were initially named “ufasomes” (“unsaturated fatty acid liposomes”).¹⁰ Later studies have shown that fatty acid vesicles can form not only from unsaturated fatty acids but also from saturated fatty acids, such as octanoic and decanoic acids.^{11–13} The mechanism of formation of fatty acid vesicles is controversial up to present.^{14–18} The simplicity of the chemical structure of fatty acids and the dynamic formation

of fatty acid vesicles have stimulated many “origin-of-life-investigators” interested in understanding the formation of the first cell-like compartments (hypothetical protocells).^{15,19}

In this paper, we investigated in detail the formation and the rheological properties of the perfluoro fatty acid (PFLA) vesicle system, with the view of exploring the comparison of hydrocarbon fatty acid vesicles. It is well known that fluorinated surfactants have attracted special interest to further develop the range of properties in surfactant mixtures because of their unique characteristics. Compared with their hydrogenated counterparts, fluorinated surfactants show much lower CMCs²⁰ and a higher surface activity and Krafft point.²¹ On the basis of the general geometrical considerations of the packing of molecules into distinct aggregate shapes,²² fluorocarbon surfactants can more easily form bilayers,^{23,24} because of a larger cross section and rigid fluorocarbon chains compared with analogous hydrocarbon chains. Consequently, perfluoro fatty acid vesicles are much more stable, which can even be kept for 2 years in the PFLA/PFL-Na/H₂O system at room temperature. Herein, the formation of perfluoro fatty acid vesicles is restricted to a rather narrow pH range, ca. 2.85–3.20 for the PFLA/PFL-Na/H₂O system and ca. 2.90–3.20 for the PFLA/PFL-Li/H₂O system, providing the

Received: March 25, 2011

Revised: June 11, 2011

Published: June 15, 2011

evidence of the “pH-sensitive vesicles”. The perfluoro fatty acid vesicle solutions show much more interesting rheological properties, such as a much higher yield stress and viscoelasticity. It is known that the Krafft points of perfluorinated surfactants are generally higher so that less than C_7 or C_8 carbon chain compounds may be used at room temperature.^{20,21} Surprisingly, the formation of vesicles can remarkably decline the Krafft points of perfluoro fatty acids and their ionized species, which may expand the development of fluorinated surfactants in both fundamental research and practical applications.

■ EXPERIMENTAL SECTION

Chemicals and Materials. Perfluorolauric acid (PFLA, 96%) was purchased from Matrix Scientific (Columbia, SC, USA). All the inorganic reagents, such as lithium hydroxide (LiOH , >99%), sodium hydroxide (NaOH , >98%), potassium hydroxide (KOH , >96%), cesium hydroxide (CsOH , >99%), etc., were purchased from Aladdin (Shanghai, China). Ultrapure water, with a resistivity of $18.25 \text{ M}\Omega \text{ cm}$, was obtained using a UPH-IV ultrapure water purifier (Chengdu Ultrapure Technology Co. Ltd., China).

Methods. The samples were prepared by mixing appropriate amounts of PFLA and MOH ($M = \text{Li}, \text{Na}, \text{K}, \text{Cs}$) in water, followed by stirring at about 70°C until all the surfactants were dissolved. All the samples were then kept at $25.0 \pm 0.1^\circ\text{C}$ for at least 2 months before their phase behavior was inspected and all the measurements were taken. Transparent, viscous, and very stable solutions were obtained.

The conductivity measurements were performed on a DDSJ-308A conductivity meter and a DJS-1C glass electrode (Shanghai Precision Scientific Instrument Co., Ltd., China) at $25.0 \pm 0.1^\circ\text{C}$. The pH values of the samples were measured on a PHS-3C precision pH meter (Shanghai Precision Scientific Instrument Co., Ltd., China) at $25.0 \pm 0.1^\circ\text{C}$. Two-phase samples of the L_1/L_α -phase and L_1/P -phase were equally stirred during the conductivity and pH measurements.

The rheological measurements were performed on a Haake RheoStress 6000 rheometer with a coaxial cylinder sensor system ($Z41^\circ \text{ Ti}$) for low viscosity samples and a core-plate system ($C35/1^\circ \text{ Ti L07116}$) for samples with high viscosity at $25.0 \pm 0.1^\circ\text{C}$ by using a Circulator HAAKE DC10 cyclic water bath (Karlsruhe, Germany). The viscoelastic properties of the samples were determined by oscillatory measurements with an amplitude sweep at a fixed frequency of 1.0 Hz performed prior to the following frequency sweep to ensure that the selected stress was in the linear viscoelastic region. The magnitudes of the complex viscosity $|\eta^*|$, the storage modulus G' , and the loss modulus G'' were then measured in the frequency range of 0.01–100 Hz.

A drop of an L_α -phase sample solution was placed on a silica wafer, and most of the colloid gel was removed using small forceps. The wafer was frozen in liquid nitrogen and placed in a vacuum extractor at $-50.0 \pm 0.1^\circ\text{C}$ for several hours. The samples on the silica wafers were observed using a Digital Instruments NanoScope III operating in tapping mode.

To characterize the structure of the L_α -phase sample solution, FF-TEM observations were performed. A small amount of the L_α -phase solution was placed on a 0.1 mm thick copper disk covered with a second copper disk. The copper sandwich with the sample solution was then immersed rapidly into the liquid ethane cooled by liquid nitrogen to freeze. They were transferred into liquid nitrogen after several seconds. The samples, after being transferred into the chamber of the freeze-etching

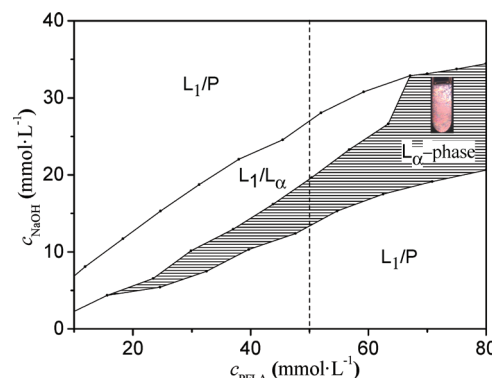


Figure 1. Phase diagram of dilute solutions for the PFLA/NaOH/H₂O system at $25.0 \pm 0.1^\circ\text{C}$. The phase denoted by “P” means precipitation, “ L_1 ” means isotropic solution, and “ L_α ” means anisotropic birefringent phase. A typical birefringent L_α -phase sample is inserted in the phase diagram.

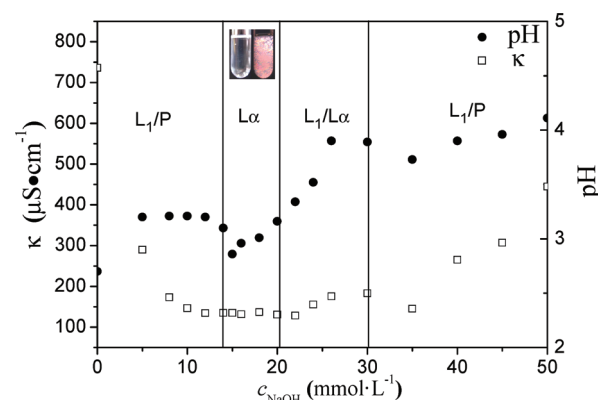


Figure 2. A section of the phase diagram of dilute solutions for the PFLA/NaOH/H₂O system with $c_{\text{PFLA}} = 50 \text{ mmol} \cdot \text{L}^{-1}$ at $25 \pm 0.1^\circ\text{C}$. A typical birefringent L_α -phase sample without (left) and with (right) crossed polarizers is inserted in the phase diagram. The conductivity data (\square) and pH values (\bullet) are given.

apparatus (Balzers BAF-400D), were fractured at a temperature and pressure of -150°C and 10–7 Pa. After being etched for 1 min, Pt-C was sprayed onto the fracture face at 45° , and then C was sprayed at 90° . The replicas were examined on a JEOL 100CX-II TEM operating at an accelerating voltage of 100 kV.

The Krafft points and the phase transition temperatures of the crystalline to liquid state were determined on a DSC-1 (Mettler Toledo, Switzerland). Samples were analyzed in aluminum pans under a flow of nitrogen and heated at $10^\circ\text{C}/\text{min}$ from 10 to 120°C , and an empty aluminum pan was used as a reference.

■ RESULTS AND DISCUSSION

Phase Behaviors of PFLA/NaOH/H₂O and PFLA/LiOH/H₂O Systems. Figure 1 presents the phase diagram of dilute solutions for the PFLA/NaOH/H₂O system at $25.0 \pm 0.1^\circ\text{C}$. The phase diagram is divided into four regions mainly. Two vast areas are inhabited by the L_1 /Precipitates (abbreviated as P) two-phase region in both PFLA-rich and (PFL-Na)-rich sides. This is because the Krafft point of PFLA is about 55.5°C^{25} and PFL-Na is higher than 70°C . However, when PFLA and NaOH are mixed together at an appropriate ratio, a transparent birefringent

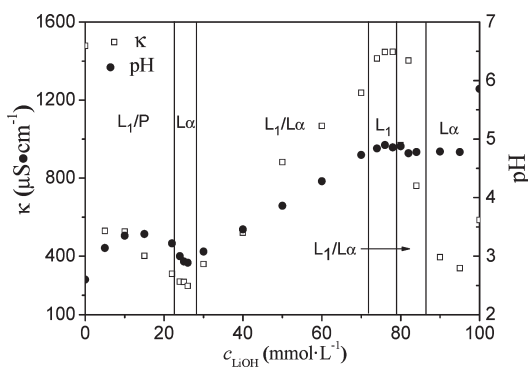


Figure 3. Phase diagram of dilute solutions for the PFLA/LiOH/H₂O system with $c_{\text{PFLA}} = 100 \text{ mmol}\cdot\text{L}^{-1}$ at $25.0 \pm 0.1^\circ\text{C}$. The conductivity data (\square) and pH values (\bullet) are also given.

L_α -phase appears at room temperature, indicating the formation of lamellar structures in solution. On the (PFLA-Na)-rich side, beside the L_1/P two-phase region and the L_α -phase area, is a transitional phase, a L_1/L_α two-phase region. In this region, the L_α -phase solution is at the bottom of the tubes, whereas the L_1 -phase solution is at the top because of the high density of the fluorinated surfactant. Herein, the Krafft point of PFLA and PFL-Na can be remarkably reduced by mixing them together at an appropriate ratio with the formation of the aggregation.

If we keep the concentration of PFLA at 50 $\text{mmol}\cdot\text{L}^{-1}$, then vary the concentration of NaOH, a section of the phase diagram (broken line in Figure 1) would be obtained, as shown in Figure 2. For the section with $c_{\text{PFLA}} = 50 \text{ mmol}\cdot\text{L}^{-1}$, one can observe, in turn, an L_1/P two-phase, an L_α -phase, an L_1/L_α two-phase, and another L_1/P two-phase. The minimum conductivity is in the L_α -phase region, then increases, expanding to both sides, which means that the L_α -phase may be the vesicle phase.²⁶ In fact, this is further indicated by AFM and FF-TEM observations rearwards. The pH values in the whole section are acidic, because perfluorocarboxylic acids can only be considered as strong acids as long as they are in the monomeric state.²⁴ In the two L_1/P two-phase regions, the pH values remain almost constant, respectively, because of their infusibility in aqueous solutions at room temperature. Unexpectedly, the pH values decrease in the L_α -phase, which range from 2.85 to 3.20; in other words, the formation of vesicles is restricted in this rather narrow pH range.

To investigate the influence of different counterions on the formation and the stability of the vesicle phase, 100 $\text{mmol}\cdot\text{L}^{-1}$ PFLA was mixed with LiOH, KOH, and CsOH at different ratios. Because of the smaller volume and higher charging density of Li⁺, pure PFL-Li forms a lamellar LLC phase in aqueous solutions, which was studied in detail in our other report. The PFLA/LiOH/H₂O mixture system can form the vesicle phase within a rather narrow pH range from 2.90 to 3.20, as shown in Figure 3. With the increase of LiOH, the vesicle phase finally transits to another L_α -phase of the lamellar LLC phase. Besides the two L_α -phase regions, an isotropic L_1 phase, a $L_1/\text{Precipitates}$ two-phase, and two L_1/L_α two-phase regions can be observed. The conductivity data decreases in the two L_α -phase regions; it is because the formation of vesicles can wrap some of the conductive ions. Meanwhile, the formation of the lamellar LLC phase remarkably increases the viscosity of the samples. However, in the case of PFLA mixed with KOH and CsOH, only precipitates are observed in aqueous solutions at any ratio, which should be

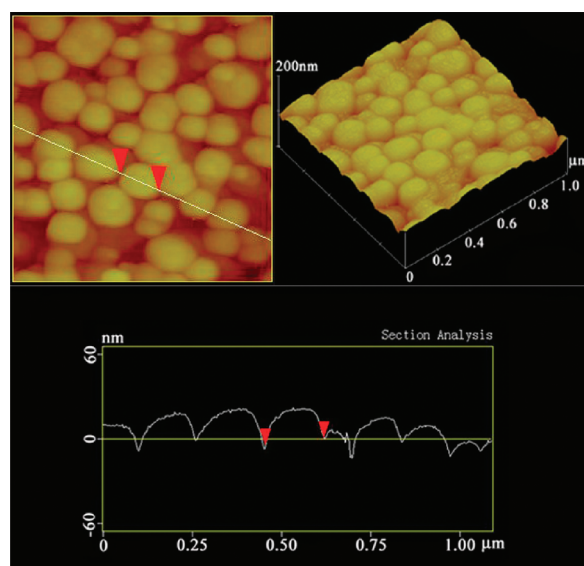


Figure 4. AFM micrographs of the L_α -phase sample with the concentration of 50 $\text{mmol}\cdot\text{L}^{-1}$ PFLA and 15 $\text{mmol}\cdot\text{L}^{-1}$ NaOH.

due to the larger volumes and lower extent of hydration than Li⁺ and Na⁺.

AFM micrographs of the L_α -phase sample, as shown in Figure 4, indicate the shriveled vesicles with diameters ranging from about 50 to 160 nm. The size of the vesicles is larger than that of FF-TEM micrographs, as shown in Figure 5, which is reasonable because the sample has been evaporated and the vesicles are shriveled. What's more, the tapping mode of AFM measurements also makes the visible size of the vesicles larger than their trim size. Herein, we should point out that the observations of AFM measurements for vesicles from surfactants in solution could be suitable for stable vesicle systems, such as fluorinated or macromolecule surfactant systems that have rigid chains.^{25,27,28}

In the next experiment, we determined the microstructures of the vesicle phase and LLC phase of PFLA/NaOH/H₂O and PFLA/LiOH/H₂O systems by FF-TEM measurements. The FF-TEM micrograph in Figure 5a clearly shows the unilamellar vesicles of the L_α -phase solution in the PFLA/NaOH/H₂O system. The small unilamellar vesicles are mainly less than 100 nm with diameters ranging from 30 to 80 nm, only half of those measured by AFM. The phase transition from the vesicle phase to the lamellar LLC phase in the PFLA/LiOH/H₂O system is determined by FF-TEM images, as shown in Figure 5b,c. Similarly, the unilamellar vesicles of the L_α -phase sample of the PFLA/LiOH/H₂O system are small, ranging from 30 to 70 nm in Figure 5b. However, the vesicles are more unstable than those of the PFLA/NaOH/H₂O system, because the higher charging density of Li⁺ screens part of the electric charge of the bilayers. With the increase of pH, the vesicle phase transits to the LLC phase, as shown in Figure 5c. It can be seen that the lattice spacing of interlayers is about 20 nm, which is determined by SAXS measurements in our other report.

Basically, lamellar phase samples (stacked lamellae and vesicles) with large sizes should show stationary birefringence; however, in our present systems, the vesicles have diameters ranging from below 100 nm (the average size of the vesicles is about 50 nm from the TEM images). Thus, the stationary



Figure 5. FF-TEM micrographs of the L_{α} -phase samples of PFLA/NaOH/H₂O and PFLA/LiOH/H₂O systems: 50 mmol·L⁻¹ PFLA and 15 mmol·L⁻¹ NaOH, vesicle phase (a), 100 mmol·L⁻¹ PFLA and 25 mmol·L⁻¹ LiOH, vesicle phase (b), and 100 mmol·L⁻¹ PFL-Li, lamellar LLC phase (c).

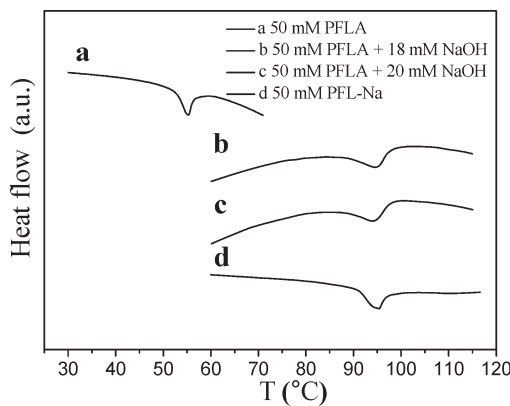


Figure 6. DSC curves of a soliquid sample of 50 mmol·L⁻¹ PFLA (a), two birefringent L_{α} -phase samples for 50 mmol·L⁻¹ PFLA + 18 mmol·L⁻¹ NaOH (b), 50 mmol·L⁻¹ PFLA + 20 mmol·L⁻¹ NaOH (c), and the soliquid sample of 50 mmol·L⁻¹ PFL-Na (d).

birefringence may not come from vesicles; that is, a solution with optically isotropic objects (vesicles) that are smaller than the wavelength of light cannot show stationary birefringence. The shown birefringence (the sample in Figure 1) may, therefore, be a different cause, which shall be further explored.

The temperature-dependent transitions of surfactant alkyl chains between various different lamellar phases have been studied by means of DSC.^{29–31} In this method, the fluorocarbon chains of PFLA and PFL-Na may be present either in the fluid state or in crystalline form in this system. A typical DSC trace of PFLA is shown in Figure 6; the Krafft point is about 55.5 °C from curve a.²⁵ However, the Krafft point of PFL-Na, which is much higher than that of PFLA, reaches 95.3 °C from curve d. Consequently, the transition temperatures of the crystalline form to the fluid state in the PFLA/NaOH/H₂O L_{α} -phase are about 94.5 and 93.9 °C (curves b and c), respectively, corresponding to the two samples of 50 mmol·L⁻¹ PFLA + 18 mmol·L⁻¹ NaOH and 50 mmol·L⁻¹ PFLA + 20 mmol·L⁻¹ NaOH. This indicates that the fluorinated alkyl chains of PFL⁻ are in the crystalline state at room temperature because of their higher rigidity compared with an analogous hydrocarbon chain.

In our present study, it is an interesting problem to know that the vesicle aggregates are influenced by stirring or mixing processes. In fact, the conclusions on the spontaneous formation of vesicles from surfactant mixtures are controversial up to present. There are still publications where the existence of vesicles as thermodynamic species is doubted and where it is assumed that, given enough time, the vesicles will transform or

condense into an L_{α} -phase,^{32,33} which means that the vesicle aggregates are greatly influenced by stirring or mixing processes.

In our present case, the stirring or mixing processes have little influence on the formation of vesicles. We observed the spontaneous formation of vesicles without stirring when the right mixing ratios of solid PFLA and PFL-Na are established in water. We mixed the two solid compounds of PFLA and PFL-Na in water with a much shorter time than the appearance of the birefringent L_{α} -phase (several days normally). The sample was at rest and does not flow at $T = 25.0 \pm 0.1$ °C for observations. We observed the appearance of the birefringent L_{α} -phase after several days; the sample solution of the birefringent L_{α} -phase can be kept for more than 2 years. Thus, we believe that the vesicles are in an equilibrium state, and it is finally shown that L_{α} -phases are indeed obtained when the two components are mixed without shear.

Rheological Properties of PFLA/NaOH/H₂O and PFLA/LiOH/H₂O Systems. The macroproperties of PFLA/NaOH/H₂O and PFLA/LiOH/H₂O systems were characterized by rheological measurements of the oscillatory sweep mode. Two typical rheograms of the oscillatory frequency sweep for two samples, 40 mmol·L⁻¹ PFLA/12 mmol·L⁻¹ NaOH and 70 mmol·L⁻¹ PFLA/21 mmol·L⁻¹ NaOH (the ratios of PFLA and PFL-Na are 7:3), are shown in Figure 7. One can see that the two samples show similar rheological properties. The complex viscosity (η^*) decreases over the whole frequency with a slope of -1 . The storage modulus (G') and loss modulus (G'') are a little dependent on frequency, and G' is much higher than G'' , indicating that the vesicle phase solutions are viscoelastic. This is different than hydrocarbon fatty acid vesicle solutions, which are not so stable and viscoelastic, because of the higher rigidity and stronger hydrophobic interaction of the fluorocarbon chain. The very high values of the storage modulus indicate that the fluorinated alkyl chains of PFL⁻ are in the crystalline state at room temperature, which is in agreement with the DSC results.

The vesicle solution of 100 mmol·L⁻¹ PFLA and 25 mmol·L⁻¹ LiOH behaves like a Bingham fluid, as shown in Figure 8a. Over the range of 0.01–100 Hz, both G' and G'' are nearly frequency-independent, and G' is about 1 order magnitude higher than G'' . The complex viscosity (η^*) of the samples linearly decreases with a slope of -1 . The gel-like lamellar LLC phase sample of 100 mmol·L⁻¹ PFL-Li also shows a highly viscoelastic response. Over the range of 0.01–100 Hz, both G' and G'' rise relaxedly with the increasing of the frequency, and G' is about 1 order magnitude higher than G'' all along from Figure 8b. One can observe that η^* of the lamellar LLC phase sample is about 1 order of magnitude higher than that of the

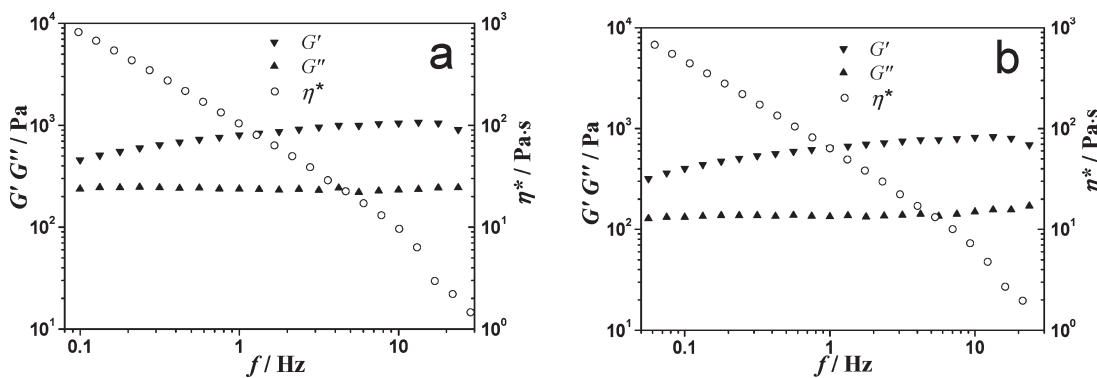


Figure 7. Typical oscillatory rheograms of the vesicle phase samples for PFLA/NaOH/H₂O systems at 25.0 ± 0.1 °C: 40 mmol·L⁻¹ PFLA and 12 mmol·L⁻¹ NaOH (a) and 70 mmol·L⁻¹ PFLA and 21 mmol·L⁻¹ NaOH (b).

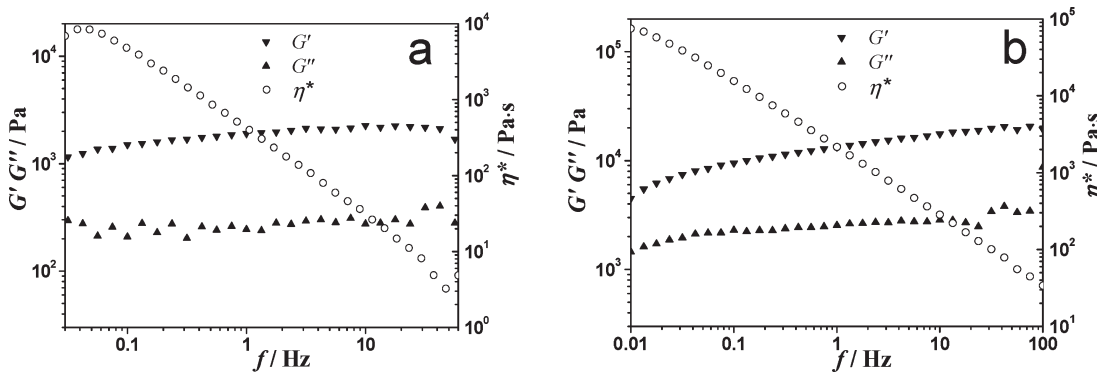


Figure 8. Typical oscillatory rheograms of the L_α-phase samples for PFLA/LiOH/H₂O systems at 25.0 ± 0.1 °C: 100 mmol·L⁻¹ PFLA and 25 mmol·L⁻¹ LiOH, vesicle phase (a) and 100 mmol·L⁻¹ PFL-Li, lamellar LLC phase (b).

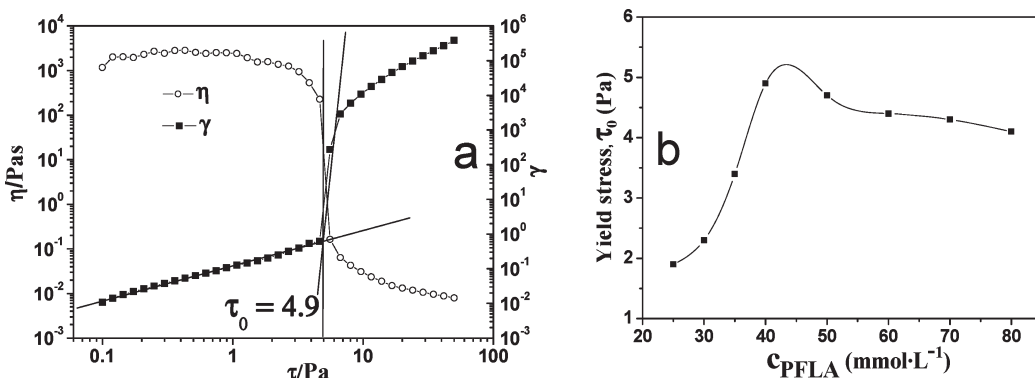


Figure 9. Determination of a yield stress of the vesicle phase sample, 40 mmol·L⁻¹ PFLA and 12 mmol·L⁻¹ NaOH at 25.0 ± 0.1 °C; the ratio of PFLA and PFL-Na is fixed at 7:3. The apparent viscosity η and deformation γ are given (a) and the yield stress against concentration of PFLA (b).

vesicle phase sample, also indicating the transition from the vesicle phase to the lamellar LLC phase.

To further explore the rheological properties of vesicle phase solutions, steady-shear rheology of samples with different concentrations of PFLA and NaOH was performed. The vesicle phase solutions of the PFLA/NaOH/H₂O system actually have a real yield stress value, as shown in Figure 9a. To determine the yield stress value, we measure the deformation (γ) and apparent viscosity (η) when the systems are exposed to increasing shear stresses from 0.1 to 50 Pa. As

shown in Figure 9a, the deformation of the vesicle phase solution can be divided into two responses, indicating that the system indeed has a yield value. At the beginning, the system responds only elastic properties, the deformation depends only on the shear stress and not on the time when the stress is applied, and the apparent viscosity is nearly stress-independent at the same time. However, when the stress increases to the yield stress value ($\tau_0 = 4.9$ Pa), the deformation increases abruptly, and the apparent viscosity descends remarkably. The system then exhibits viscous properties, the slope of

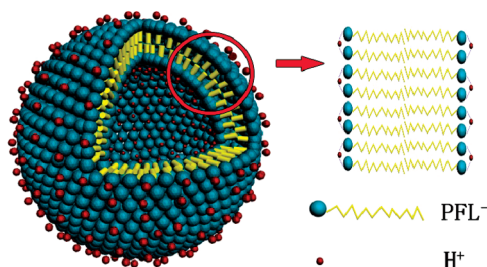


Figure 10. Schematic view of the self-assembly of PFL^- and H^+ into vesicles through hydrogen bonds.

deformation increases, and the apparent viscosity linearly decreases, indicating that the solution starts to flow and shear thinning. The high yield values of the vesicle phase solution indicate the dense packing of small perfluoro fatty acid vesicles.

The yield stress value depends on the total surfactant concentration, as demonstrated in Figure 9b. When the ratio of PFLA and PFL-Na is fixed at 7:3, then the total surfactant concentration (c_{PFLA}) is varied, a series of yield values are obtained. Under very low concentration, vesicles no longer densely packed can easily move around each other under shear flow, so the yield value disappears.³⁴ The yield value increases rapidly before $42 \text{ mmol} \cdot \text{L}^{-1}$ but decreases relaxedly after $42 \text{ mmol} \cdot \text{L}^{-1}$ with the increase of the concentration of PFLA. We suspect that the elasticity of the system is increasing with the increase of c_{PFLA} before $42 \text{ mmol} \cdot \text{L}^{-1}$, because of the formation of more numerous vesicles. However, the number of vesicles is not limitless, so the viscosity of the system will increase after $42 \text{ mmol} \cdot \text{L}^{-1}$, with solubilizing more surfactants to the vesicles, and the elasticity of the system will decrease.

Proposal Mechanism of pH-Sensitive Vesicles of PFLA and Its Salts. Until now, the mechanism of formation of fatty acid vesicles is disputable. Walde et al.^{15,16,35} summarized that fatty acid vesicles, which are actually “fatty acid/soap vesicles”, always contain two types of amphiphiles, the nonionized, neutral form and ionized form, and their ratio is critical for the vesicle formation and stability. However, Haines¹⁴ reported that the protonated fatty acids form stable acid–anion pairs with deprotonated fatty acids through unusually strong hydrogen bonds. Under an appropriate pH value, the stable acid–anion dimers can form fatty acid vesicles. They considered that the anionic headgroups of the vesicles of energy-transducing membranes have the capacity to bind and conduct protons along the membrane surface. In any case, the pH value and the ratio of fatty acid/soup play an important role in the formation and stability of vesicles. On the basis of the general geometrical considerations of the packing of molecules into distinct aggregate shapes,²¹ surfactants can form bilayers when the packing parameter p is in the range of $1/2 \leq p \leq 1$ ($p = (v)/(al)$, in which a is the interfacial area occupied by a surfactant headgroup and l and v are the length and the volume of the hydrophobic group, respectively). Both of the above-mentioned two considerations can change the packing parameter p , which is beneficial to the formation of vesicles.

According to experimental data and the above analysis, a proposed mechanism of self-assembly of PFL^- and H^+ into vesicles is shown in Figure 10. As shown in the model, two protonated PFL^- ions form stable dimers through strong hydrogen bonds first. The single negatively charged dimers then

self-assemble to bilayer membranes. Depending on a competitive balance between attractive hydrophobic interaction and repulsive electrostatic force, stable small unilamellar vesicles form under an appropriate ratio of fatty acid/soup. The mechanism of perfluorocarboxylic acid vesicle formation has a better chance to follow Haines’ theory, which is because (i) the perfluorocarboxylic acids can only be considered as strong acids as long as they are in the monomeric state,²⁴ so one believes perfluorocarboxylic acids are absolutely ionized when they are dissolving in water, (ii) hydrogen bonds between perfluorocarboxylic headgroups are inevitable under an acidic pH value, and (iii) our experimental results indicate that the pH values decrease in the vesicle phase, which range from 2.85 to 3.20.

Consequently, with the formation of vesicles, the PFLA with a fairly high Krafft point can dissolve into aqueous solution, and excess H^+ ions are released to the bulk. This is the reason why the pH values decrease in the vesicle phase. However, with the increase of pH value, the vesicles will wear away because the hydrogen bonds between perfluorocarboxylic headgroups are destroyed. In other words, the vesicles of PFLA and its salts in aqueous solutions are pH-sensitive.

CONCLUSIONS

In the present article, we have investigated in detail the phase behaviors and rheological properties of PFLA/PFL-Na/ H_2O and PFLA/PFL-Li/ H_2O systems. Similar to hydrocarbon fatty acid vesicles, the formation of perfluoro fatty acid vesicles is restricted to a rather narrow pH range (ca. 2.85–3.20 in the PFLA/PFL-Na/ H_2O system and ca. 2.90–3.20 in the PFLA/PFL-Li/ H_2O system), so they are “pH-sensitive”. Because of the differences between fluorocarbon and hydrocarbon chains, perfluorocarboxylic acid vesicles are more stable. The system of perfluoro fatty acid vesicles exhibits a much more interesting rheological behavior, compared to hydrocarbon fatty acid vesicles. For instance, the perfluoro fatty acid vesicle solutions show a much higher yield stress and viscoelasticity, which depend on two factors: (i) the fluorinated alkyl chains of PFL^- , which are in the crystalline state at room temperature because of their rigid chains compared to analogous hydrocarbon chains, and (ii) the packing of the vesicles, which is very dense. The mechanism of perfluorocarboxylic acid vesicle formation has a better chance to follow Haines’ theory: the protonated PFL^- ions first form stable dimers through strong hydrogen bonds and then self-assemble to vesicles through attractive hydrophobic interaction and repulsive electrostatic force.

AUTHOR INFORMATION

Corresponding Author

*E-mail: jhao@sdu.edu.cn. Fax: +86-531-88564750.

ACKNOWLEDGMENT

The authors thank the NSFC (Grant No. 21033005) and the National Basic Research Program of China (973 Program, 2009CB930103) for financial support.

REFERENCES

- (1) Mukerjee, P.; Yang, A. Y. *S. J. Phys. Chem.* **1976**, *80*, 1388–1390.
- (2) Li, F.; Li, G.; Chen, J. *Colloids Surf., A* **1998**, *145*, 167–174.

- (3) Kondo, Y.; Yoshino, N. *Curr. Opin. Colloid Interface Sci.* **2005**, *10*, 88–93.
- (4) Kaler, E. W.; Murthy, A. K.; Rodriguez, B. E.; Zasadzinski, J. A. N. *Science* **1989**, *245*, 1371–1374.
- (5) Herrington, K. L.; Kaler, E. W.; Miller, D. D.; Zasadzinski, J. A. N.; Chiruvolu, S. *J. Phys. Chem.* **1993**, *97*, 13792–13802.
- (6) Horbaschek, K.; Hoffmann, H.; Thunig, C. *J. Colloid Interface Sci.* **1998**, *206*, 439–456.
- (7) Zemb, Th.; Dubois, M.; Demé, B.; Gulik-Krzywicki, T. *Science* **1999**, *283*, 816–819.
- (8) Li, H.; Hao, J. *J. Phys. Chem. B* **2008**, *112*, 10497–10508.
- (9) Dong, R.; Hao, J. *Chem. Rev.* **2010**, *110*, 4978–5022.
- (10) Gebicki, J. M.; Hicks, M. *Nature* **1973**, *243*, 232–234.
- (11) Hargreaves, W. R.; Deamer, D. W. *Biochemistry* **1978**, *17*, 3759–3768.
- (12) Fontell, K.; Mandell, L. *Colloid Polym. Sci.* **1993**, *271*, 974–991.
- (13) Morigaki, K.; Walde, P.; Misran, M.; Robinson, B. H. *Colloids Surf., A* **2003**, *213*, 37–44.
- (14) Haines, T. H. *Proc. Natl. Acad. Sci. U.S.A.* **1983**, *80*, 160–164.
- (15) Morigaki, K.; Walde, P. *Curr. Opin. Colloid Interface Sci.* **2007**, *12*, 75–80.
- (16) Kanicky, J. R.; Shah, D. O. *Langmuir* **2003**, *19*, 2034–2038.
- (17) Feinstein, M. E.; Rosano, H. L. *J. Phys. Chem.* **1969**, *73*, 601–607.
- (18) Berclaz, N.; Blöchliger, E.; Müller, M.; Luisi, P. L. *J. Phys. Chem. B* **2001**, *105*, 1065–1071.
- (19) Walde, P. *Origins Life Evol. Biospheres* **2006**, *36*, 109–150.
- (20) Shinoda, K.; Hato, M.; Hayashi, T. *J. Phys. Chem.* **1972**, *76*, 909–914.
- (21) Kunieda, H.; Shinoda, K. *J. Phys. Chem.* **1976**, *80*, 2468–2470.
- (22) Israelachvili, J.; Mitchell, D. J.; Ninham, B. W. *J. Chem. Soc., Faraday Trans. 2* **1976**, *72*, 1525–1568.
- (23) Fontell, K.; Lindman, B. *J. Phys. Chem.* **1983**, *87*, 3289–3297.
- (24) Hoffmann, H.; Würtz, J. *J. Mol. Liq.* **1997**, *72*, 191–230.
- (25) Long, P.; Hao, J. *Soft Matter* **2010**, *6*, 4350–4356.
- (26) Valiente, M.; Thunig, C.; Munkert, U.; Lenz, U.; Hoffmann, H. *J. Colloid Interface Sci.* **1993**, *160*, 39–50.
- (27) Chen, Q.; Schonherr, H.; Vancso, G. J. *Soft Matter* **2009**, *5*, 4944–4950.
- (28) Yang, M.; Wang, W.; Yuan, F.; Zhang, X.; Li, J.; Liang, F.; He, B.; Minch, B.; Wegner, G. *J. Am. Chem. Soc.* **2005**, *127*, 15107–15111.
- (29) Vautrin, C.; Dubois, M.; Zemb, Th.; Schmölzer, St.; Hoffmann, H.; Gradielski, M. *Colloids Surf., A* **2003**, *217*, 165–170.
- (30) Hao, J.; Hoffmann, H. *Curr. Opin. Colloid Interface Sci.* **2004**, *9*, 279–293.
- (31) Zemb, Th.; Dubois, M. *Aust. J. Chem.* **2003**, *56*, 971–979.
- (32) Horbaschek, K.; Hoffmann, H.; Hao, J. *J. Phys. Chem. B* **2000**, *104*, 2781–2784.
- (33) Laughlin, R. G. *Colloids Surf., A* **1997**, *128*, 27–38.
- (34) Hoffmann, H.; Thunig, C.; Schmiedel, P.; Munkert, U. *Langmuir* **1994**, *10*, 3972–3981.
- (35) Morigaki, K.; Dallavalle, S.; Walde, P.; Colonna, S.; Luisi, P. L. *J. Am. Chem. Soc.* **1997**, *119*, 292–301.